To be published in the proceedings of the
18th International Conference on Port and Ocean
Engineering under Arctic Conditions (POAC),
26 through 30 June 2005, Potsdam, NY, USA

ON THE RELATIONSHIP BETWEEN EFFECTIVE AND TOTAL PORE SPACE IN SEA ICE

Chris Petrich[1] **and Pat J. Langhorne**[1]

[1]**University of Otago, Physics Department, Dunedin, New Zealand**

ABSTRACT

We present a Monte Carlo percolation model to estimate the relationship between effective (connected) pore space and total pore space in sea ice. The percolation model discriminates between regions of ice platelets and brine layers to typify a columnar crystal structure. It is found that the dimensions of the computational domain and the critical porosity are quantitatively consistent with measurements from the literature for sea ice. The cluster size distribution produced by the model is further similar to the inclusion size distribution observed in sea ice. Agreement and differences are discussed.

BRINE LAYER MODEL

We seek a relationship between total porosity f_t and effective porosity f_e using a simple Monte Carlo percolation model. Pockets, representing brine inclusions, are added into a domain, representing sea ice, and the relationship between total porosity and effective porosity is evaluated. Total porosity is the volume fraction of all inclusions of the material, while effective porosity is the pore space of the infinite cluster (Stauffer and Aharony, 1992), i.e. the volume of inclusions that are connected to the periphery of a sample of infinite size.

Concepts of percolation theory have previously been applied to sea ice (Golden et al., 1998) to explain the origin of the critical porosity (percolation threshold) f_c of sea ice, i.e. the porosity below that sea ice becomes virtually impermeable to fluid flow. Cox and Weeks (1975) report that no brine drainage from sea ice was observed for total porosities below $f_c = 0.05$. However, common two and

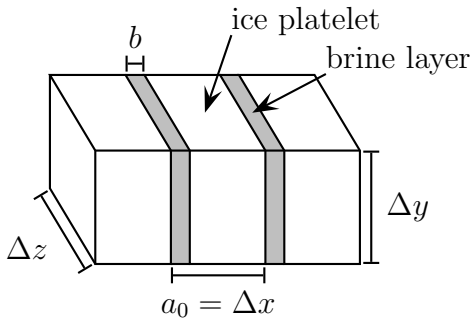

Figure 1: Schematic of the periodic stacking of brine layers and ice platelets in sea ice (sandwich model). The brine layer width is b, and the platelet spacing is $a_0 = \Delta x$.

three dimensional systems of randomly distributed conducting circles or spheres exhibit much larger critical porosities, i.e. respectively $f_c \approx 0.676$ and $f_c \approx 0.290$ (Baker et al., 2002). The precise value of the critical porosity has been found to depend on pocket shape (Garboczi et al., 1995), pocket distribution (Gaonac'h et al., 2003), and system dimension (Stauffer and Aharony, 1992). For example, a reduction of the three dimensional percolation threshold to a value observed in sea ice is expected in media with randomly oriented ellipsoid pockets, approximately 15 times longer than wide, distributed throughout the domain (Garboczi et al., 1995). Golden et al. (1998) choose a different explanation for the low percolation threshold in sea ice, exploiting the size ratio of sea ice platelets and brine pockets to account for this observation. In order to quantify their argument they apply a compressed powder model (Kusy, 1977). This compressed power model has been shown to be the limiting case of a simpler and more rigorous approach suggested by Janzen (1975) (Janzen, 1980). Janzen (1975) notes that percolation can sometimes be treated by considering only the volume to which the pores have random access. The result seems to be independent of the shape of the excluded volume (Janzen, 1975).

Analytical considerations

Applying Janzen (1975) to columnar sea ice, we discriminate between a brine layer of width b that contains ice and brine pockets, and pure ice platelets of width $a_0 - b$, to which brine inclusions have no random access (Figure 1). This picture is not applicable in the limit of high porosity, i.e. when b is variable, for example in the skeletal layer. We will account for this latter situation below, however.

Using percolation theory in infinite systems, a scaling relationship exists between the effective porosity in the brine layer, f_{be}, and the total porosity in that layer, f_{bt},

(1) $\quad f_{be} \propto (f_{bt} - f_{bc})^{\beta} \quad \text{for} \quad f_{bt} \gtrsim f_{bc},$

where f_{bc} is the critical porosity of the brine layer, and β is some ("critical") exponent. Equation (1) is defined for f_{bt} larger but similar to f_{bc} (Stauffer and Aharony, 1992). The effective brine layer porosity f_{be} is zero for total brine layer porosities below the critical brine layer porosity. It is further known that the exponent $\beta = 5/36 \approx 0.139$ and $\beta \approx 0.41$ in two and three dimensional systems, respectively (Stauffer and Aharony, 1992; Sahimi, 1993). However, percolation theory does not predict the constant of proportionality.

Assuming that no pockets can be present in the ice platelets, simple relationships exist between brine layer porosity and total porosity from geometric considerations, i.e.

$$(2) \quad f_t = \frac{b}{a_0} f_{bt}, \quad f_e = \frac{b}{a_0} f_{be}, \quad f_c = \frac{b}{a_0} f_{bc}.$$

Substituting (2) into (1), the expected relationship between effective porosity and total porosity of sea ice is

$$(3) \quad f_e \propto \left(\frac{b}{a_0}\right)^{1-\beta} (f_t - f_c)^{\beta}.$$

Equation (3) suggests that the relationship between effective porosity f_e and total porosity f_t depends on the microstructure of sea ice.

Since the constant of proportionality in (3) is still undetermined, we will find a possible relationship between f_t and f_e from a Monte Carlo model, and compare that relationship with (3).

Description of the Monte Carlo model

In our model, the sea ice sheet is a cubical domain that is riddled with pockets shaped as rectangular boxes. Rectangular boxes are chosen as the exact calculation of total and effective volumes is possible and even trivial. Pockets are aligned with the sides of the domain. The model is continuous, which means that no grid is used. In the course of the simulation, pockets are sequentially inserted into the domain at random locations[1]. The pockets have a "soft core", i.e. they may overlap. If pockets overlap they form a cluster. After a pocket has been added the total porosity f_t of the domain is calculated, accounting for pocket overlap, and the total volume that is occupied by clusters that connect to both the top boundary and the bottom boundary is determined (y–direction). The latter volume is the effective porosity f_e. The domain is periodic in x and in z–directions in order to reduce finite size effects. The computational algorithm is described in more detail by Petrich (2005).

[1]The random number generator used is *Mersenne Twister* (Matsumoto and Nishimura, 1998), implemented as `mt19937ar.c`, 26 January, 2002, by Makoto Matsumoto and Takuji Nishimura with 53 bit number generation due to Isaku Wada.

The Monte Carlo model is validated by determining the critical porosity in both two and three dimensions. As shown by Petrich (2005), the critical porosities for squares in two dimensions and for cubes in three dimensions are determined to be $f_c = 0.667$ and $f_c = 0.277$, respectively. These results are in excellent agreement with the results of Baker et al. (2002).

The platelet structure of sea ice is approximated by a sandwich layer model of alternating brine layers and ice platelets as illustrated in Figure 1 and described by Perovich and Gow (1996). An attempt is made to add pockets to the domain at random locations. If they fall completely into a brine layer, treatment is as described above. If they partially or completely fall into the domain of a platelet, however, they are added only if they connect to an existing cluster.

The physical significance of this difference is that we allow clusters to come into existence and to grow in brine layers, while, in platelets, clusters are only allowed to grow. The cluster creation is similar to an observation of Perovich and Gow (1996). At first glance they find, upon warming, that brine inclusions seem to appear at random locations. Closer investigation, however, revealed that inclusions already existed at those locations, but that their sizes were below the detection limit. A similar observation has been made by Eicken et al. (2000). The insertion of pockets into the brine layers is therefore equivalent to pre–existing brine inclusions reaching the detection limit. On the other hand, the prohibition of pocket insertion in the platelet regions means that the only way for inclusions to interfere with the platelets is by melting or dissolving into them.

We anticipate that this model will produce a percolation threshold f_c that can be calibrated by adjusting brine layer thickness b and platelet spacing a_0 of the stacking sequence in Figure 1 following (2). Further, we expect that the model will yield the desired relationship $f_e = f_t$ for $f_t \to 1$, i.e. in the skeletal layer.

Relationship between effective porosity and total porosity

Figures 2(a) and (b) show the relationship between effective porosity f_e and total porosity f_t for three example calculations: a two–dimensional domain of 2000×2000, a three–dimensional domain of $200 \times 200 \times 200$, and a sandwich domain of $a_0 = \Delta x = 1000$, $b = 195.1$, and $\Delta y = \Delta z = 200$, respectively. The relationship between a_0 and b has been selected to yield a critical porosity of $f_c = 0.054$, which is the critical porosity that has been used in the permeability function of Petrich et al. (2004) and Petrich et al. (submitted).

It is clear from Figure 2(a) that a relationship $f_e = f_t$ is approached for $f_t \gg f_c$. Figure 2(b) shows the relationship between f_e and $f_t - f_c$. From percolation theory it is expected that

$$f_e = \alpha \, (f_t - f_c)^{\beta} \quad \text{for} \quad f_t \gtrsim f_c, \tag{4}$$

where α is a constant of proportionality (cf. equation (3)). The straight portions of the double logarithmic plot of Figure 2(b) can be approximated by the power

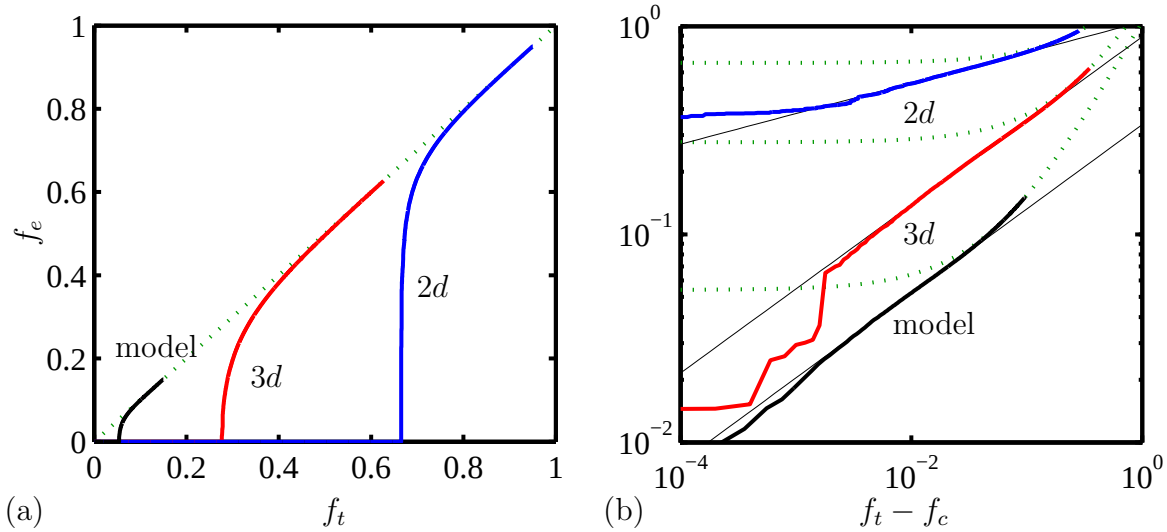

Figure 2: Effective porosity f_e as a function of (a) total porosity f_t, and (b) total porosity above critical porosity $f_t - f_c$ for the cases of two–dimensional ($2d$), three-dimensional ($3d$), and sandwich model domains. The dotted lines follow $f_e = f_t$. The critical porosity f_c appropriate for each domain is used in (b). The thin lines in (b) are the best fit power law functions (4) with parameters listed in Table 1. Note the different scales in (a) and (b).

Table 1: Parameters α and β determined from the percolation model in domains 2000×2000 ($2d$, squares), $200 \times 200 \times 200$ ($3d$, cubes), and in the sandwich domain ($a_0 = 1000$, $b = 195.1$, $\Delta y = \Delta z = 200$).

	$2d$	$3d$	sandwich
fit interval $f_t - f_c$	$[2, 6] \times 10^{-2}$	$[1, 10] \times 10^{-2}$	$[3, 30] \times 10^{-3}$
α	1.050	0.890	0.337
β	0.149	0.404	0.406
f_c	0.667	0.277	0.0540

law (4) with best–fit parameters summarised in Table 1. The parameters α and β are determined from averages of three runs, each producing a critical porosity within ± 0.001 of the expected value for the cases of two and three dimensions. The parameters for α, β, and f_c for the sandwich model are averages of 16 runs. We see that the exponents β are close to the expectations for two and three–dimensional systems of 0.139 and 0.41, respectively. Since finite size effects may still be present, and since the values of the fit parameters depend slightly on the choice of the interval used for fitting (given in Table 1), we accept this discrepancy between the current and the literature values.

With parameters from Table 1 for the sandwich model, the relationship be-

tween effective and total porosities is

$$(5)\quad f_e = \begin{cases} 0 & \text{for} \quad f_t \le 0.054, \\ 0.34\,(f_t - 0.054)^{0.41} & \text{for} \quad 0.054 < f_t \le 0.09, \\ f_t & \text{for} \quad 0.09 < f_t, \end{cases}$$

where $f_t = 0.09$ is the porosity at which the discontinuity in f_e is minimised. (Equation (5) has a discontinuity in f_e of 3×10^{-3} at $f_t = 0.09$.)

Using α, β, and $f_{bc} = f_c = 0.277$ determined for the three–dimensional system, and $b = 195.1$ and $a_0 = 1000$ from the sandwich model it is expected from (2) and (3) that

$$(6)\quad f_e = \alpha \left(\frac{b}{a_0}\right)^{1-\beta} \left[f_t - \frac{b}{a_0} f_{bc}\right]^{\beta},$$

$$(7)\quad f_e = 0.336\,(f_t - 0.054)^{0.404}.$$

Parameters in (5) and (7) differ by less than 0.5 % for $f_t \gtrsim 0.054$, which confirms the consistency of analytical and Monte Carlo calculations. Since we neglected dissolution of platelets in the derivation of (7), this indicates that the simulated dissolution of ice platelets (i.e. clusters growing into platelets) is slow at $f_t < 0.09$.

Discussion of model parameters a_0 and b

We have selected a ratio between brine layer width and platelet spacing of $b/a_0 = 195.1/1000$ that results in a critical porosity of 0.054 for the sandwich model. We will now check whether this ratio is realistic for sea ice.

Assuming a brine layer width of $b = 70\,\mu$m (the minimum brine layer width before the layer breaks down into brine tubes (Anderson and Weeks, 1958)), the question is whether a platelet spacing of $a_0 = 70\,\mu\text{m} \times 1000/195.1 = 360\,\mu$m is a reasonable value for sea ice. The functional descriptions of Lofgren and Weeks (1969) and Nakawo and Sinha (1984) show that a platelet spacing of $a_0 = 360\,\mu$m can be expected at a growth velocity $v = 2.8 \times 10^{-7}\,\text{m s}^{-1}$, which is a reasonable growth velocity for sea ice.

Approximation of the best fit curve

We have established that the relationship between effective and total porosity can be approximated by

$$(8)\quad f_e = \begin{cases} \alpha(f_t - f_c)^{\beta} & \text{for} \quad f_c < f_t \le f_x, \\ f_t & \text{for} \quad f_x < f_t, \end{cases}$$

where (8) and the first derivative are continuous at a transfer porosity f_x. We therefore possess enough information to calculate α and f_x directly from f_c and β. From the continuity of f_e at f_x it follows that

$$(9)\quad f_x = \alpha(f_x - f_c)^{\beta},$$

and from the continuity of the first derivative at f_x

$$(10)\quad 1 = \alpha\beta(f_x - f_c)^{\beta-1}.$$

Dividing (10) by (9) we find

$$(11)\quad f_x = \frac{f_c}{1-\beta},$$

and substituting (11) into (10) we further see that

$$(12)\quad \alpha = \frac{1}{\beta}\left(f_c\frac{\beta}{1-\beta}\right)^{1-\beta}.$$

For a random percolating system in three dimensions ($\beta = 0.41$) with $f_c = 0.054$ we can calculate from (11) and (12) that $\alpha = 0.352$ and $f_x = 0.0915$, which is in agreement with (5). In the two ($\beta = 0.139$, squares $f_c = 0.667$) and three ($\beta = 0.41$, cubes $f_c = 0.277$) dimensional cases we have $\alpha = 1.056$ and $\alpha = 0.923$, respectively (cf. Table 1).

Experimental data relating effective porosity to total porosity have been obtained for compressed calcite aggregates (Zhang et al., 1994). Comparing measurements of total and effective porosity, Zhang et al. find that $f_e = f_t$ for high porosities, but deviates from equality for $f_t < f_x = 0.07$. They further note that the effective porosity vanishes for total porosities below $f_t \leq f_c = 0.04$. While they do not discuss the relationship between f_c and f_x, we note that their observation is consistent with (11) with $\beta = 0.41$.

INCLUSION SIZE DISTRIBUTION IN THREE DIMENSIONS

The cluster size distribution of the sandwich model is approximated well by the cluster size distribution in three dimensions (Petrich, 2005). At low porosities it assumes a lognormal distribution, that slowly widens and shifts towards larger mean cluster sizes, until a power law distribution is attained at the critical porosity of about 0.28. For the largest porosities the distribution follows a non–normalised lognormal distribution.

Figures 3(a) and (b) show the cluster size distributions of a domain $200\times200\times200$ at $f_t = 0.20 < f_c$ ($N = 570000$ clusters) and $f_t = f_c = 0.276$ ($N = 370000$ clusters), respectively. The dotted lines follow the function

$$(13)\quad \mathrm{PDF}(v) = v^{-2.1},$$

where v is the cluster volume in multiples of pocket volumes. An exponent of approximately -2.1 is expected at the percolation threshold (Gaonac'h et al., 2003). An exponent of -2.1 has been found by Klug et al. (2002) for example to describe the pore structure of volcanic products (Gaonac'h et al., 2003).

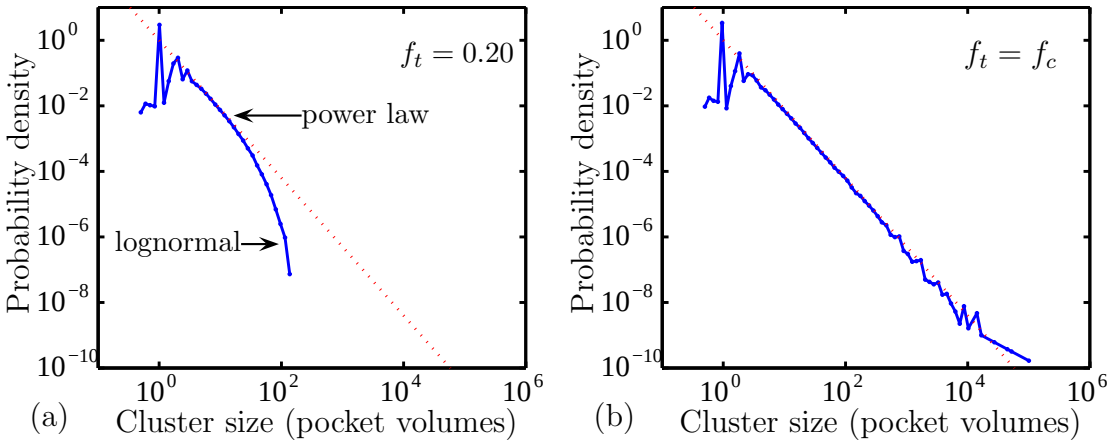

Figure 3: Cluster size distribution of a domain $200 \times 200 \times 200$ (a) below the critical porosity, $f_t = 0.200$, (b) at the critical porosity, $f_t = f_c = 0.276$. Similar distributions are found for the sandwich model.

The number density distribution (inclusions per area), $N(A)$, of brine inclusions in sea ice with respect to horizontal inclusion area, A, shown by Cole et al. (2004), and the superposition of data of Perovich and Gow (1996) and Light et al. (2003) shown by Light et al. (2003) resemble a power law distribution and a lognormal distribution at small and large inclusion sizes, respectively (cf. Figure 3(a)). The number density distribution (inclusions per volume), $N(V)$, of brine inclusions in sea ice with respect to inclusion volume, V, used by Light et al. (2004) at $-15\,^{\circ}\mathrm{C}$ follows a power law with exponent -1.1 that changes to -1.4 upon warming to $-1\,^{\circ}\mathrm{C}$, when the merging of inclusions is considered.

SUMMARY AND CONCLUSION

By assuming a three–dimensional percolation system ($\beta = 0.41$) and a critical porosity, f_c, equations (8), (11), and (12) define an approximation for the relationship between effective and total porosity for $f_t > f_c$ for an infinite random porous medium. Pocket shape and crystal structure are accounted for by f_c (equation (2)). The relationship is consistent with the Monte Carlo model of this paper. Although the model seems to be applicable to some porous media, its validity for sea ice still needs to be tested, particularly since the effective porosity derived for infinite porous media may differ from that for media of finite size. The Monte Carlo model produces cluster size distributions below the critical porosity ($f_t < f_c$) that are qualitatively consistent with sea ice measurements from the literature.

ACKNOWLEDGEMENTS

This research was funded by the Foundation for Research, Science and Technology, New Zealand. The authors wish to thank Peter Hahn and Ilse Petrich for

their technical support in the preparation of this manuscript. CP was financially supported by a postgraduate scholarship of the University of Otago and by the Beverly Fund of the University of Otago.

REFERENCES

Anderson, D. L., and W. F. Weeks (1958). A theoretical analysis of sea ice strength. American Geophysical Union, Transactions, 39(4), 632–640.

Baker, D. R., G. Paul, S. Sreenivasan, and H. E. Stanley (2002). Continuum percolation threshold for interpenetrating squares and cubes. Physical Review E, 66, 046136.

Cole, D. M., H. Eicken, K. Frey, and L. H. Shapiro (2004). Observations of banding in first–year Arctic sea ice. Journal of Geophysical Research, 109, C08012. doi: 10.1029/2003JC001993.

Cox, G. F. N., and W. F. Weeks (1975). Brine drainage and initial salt entrapment in sodium chloride ice. Research Report 345. Cold Regions Research and Engineering Laboratory. Hanover, NH, USA.

Eicken, H., C. Bock, R. Wittig, H. Miller, and H.-O. Poertner (2000). Magnetic resonance imaging of sea–ice pore fluids: Methods and thermal evolution of pore microstructure. Cold Regions Science and Technology, 31, 207–225.

Gaonac'h, H., S. Lovejoy, and D. Schertzer (2003). Percolating magmas and explosive volcanism. Geophysical Research Letters, 30(11), 1559. doi: 10.1029/2002GL016022.

Garboczi, E. J., K. A. Snyder, J. F. Douglas, and M. F. Thorpe (1995). Geometrical percolation–threshold of overlapping ellipsoids. Physical Review E, 52(1), 819–828. Part B.

Golden, K. M., S. F. Ackley, and V. I. Lytle (1998). The percolation phase transition in sea ice. Science, 282(5397), 2238–2241.

Janzen, J. (1975). On the critical conductive filler loading in antistatic composites. Journal of Applied Physics, 46(2), 966–969.

Janzen, J. (1980). Short derivation of the influence of particle size ratio on the conductivity threshold in binary aggregates. Journal of Applied Physics, 51(4), 2279–2280.

Klug, C., K. V. Cashman, and C. R. Bacon (2002). Structure and physical characteristics of pumice from the climatic eruption of Mount Mazama (Crater Lake), Oregon. Bulletin of Volcanology, 64, 486–501.

Kusy, R. P. (1977). Influence of particle–size ratio on continuity of aggregates. Journal of Applied Physics, 48(12), 5301–5305.

Light, B., G. A. Maykut, and T. C. Grenfell (2003). Effects of temperature on the microstructure of first–year Arctic sea ice. Journal of Geophysical Research, 108(C2). doi:10.1029/2001JC000887.

Light, B., G. A. Maykut, and T. C. Grenfell (2004). A temperature–dependent, structural–optical model of first–year sea ice. Journal of Geophysical Research, 109(C6), C06013.

Lofgren, G., and W. F. Weeks (1969). Effect of growth parameters on substructure spacing in NaCl ice crystals. Journal of Glaciology, 8(52), 153–164.

Matsumoto, M., and T. Nishimura (1998). Mersenne Twister: A 623–dimensionally equidistributed uniform pseudorandom number generator. ACM Transactions on Modeling and Computer Simulation, 8(1), 3–30.

Nakawo, M., and N. K. Sinha (1984). A note on brine layer spacing of first–year sea ice. Atmosphere–Ocean, 22(2), 193–206.

Perovich, D. K., and A. J. Gow (1996). A quantitative description of sea ice inclusions. Journal of Geophysical Research, 101(C8), 18,327–18,343.

Petrich, C. (2005). Growth, structure, and desalination of refreezing cracks in sea ice. Ph.D. thesis. University of Otago. Dunedin, New Zealand.

Petrich, C., P. J. Langhorne, and Z. Sun (2004). Numerical simulation of sea ice growth and desalination. Proceedings of the 17th IAHR International Symposium on Ice, vol. 3. All–Russian Research Institute of Hydraulic Engineering (VNIIG), St. Petersburg, Russian Federation. In press.

Petrich, C., P. J. Langhorne, and Z. F. Sun (submitted). Modelling the interrelationships between permeability, effective porosity and total porosity in sea ice. submitted manuscript, 2005.

Sahimi, M. (1993). Nonlinear transport process in disordered media. AIChE Journal, 39(3), 369–386.

Stauffer, D., and A. Aharony (1992). Introduction to Percolation Theory. 2nd ed.. Taylor and Francis, London, UK.

Zhang, S., M. S. Paterson, and S. F. Cox (1994). Porosity and permeability evolution during hot isostatic pressing of calcite aggregates. Journal of Geophysical Research, 99(B8), 15,741–15,760.